THE

PHYSICAL REVIEW

A journal of experimental and theoretical physics established by E. L. Nichols in 1893

SECOND SERIES, VOL. **165**, NO. 2 — 10 JANUARY 1968

New Satellite Structure of Nd^{3+} Ions in Rare-Earth Trichlorides*

G. A. PRINZ† AND E. COHEN‡

Department of Physics, The Johns Hopkins University, Baltimore, Maryland

(Received 25 July 1967)

High-resolution, low-temperature absorption spectra of Nd^{3+} in various rare-earth trichlorides have been obtained in the region 4000–9000 Å. Detailed Zeeman studies were made in fields up to 36 kOe. The study concerns the properties of the sharp satellites separated from the electronic transitions by energies of 0.1 to 20 cm^{-1}. The dependence of these satellites upon host lattice and controlled impurities was investigated. The detailed structure of the satellites indicates near-neighbor interactions between the rare-earth ions. It is probable that the satellites are due to Nd^{3+} ions in distorted sites near crystal imperfections, in particular, dislocations.

I. INTRODUCTION

IT is well known that the optical spectra of the rare-earth (RE) salts are rich in satellites accompanying the electronic transitions. A common type, vibronic transitions, occurs when lattice vibrations are superimposed on the electronic transition. These are generally distinguished from other satellites by their large energy separations, diffuseness, low intensity, and Zeeman effect. The very low ordering temperatures of $RECl_3$ prohibit, in general, the observation of satellites due to excitation of magnons.

Also known are cases in which the RE occupies distinct sites in the crystal, each site giving rise to its own spectrum. These distinctions can arise from inequivalent sites, charge compensation, or pair interaction. The last of these can give rise to splitting of the electronic transitions (~ 1 cm^{-1} in $RECl_3$) and well-isolated lines due to the absorption of one quantum by the system of two coupled ions going through simultaneous electronic transitions. All these types can be explained, using crystal-field theory as a starting point.

Besides these, there remains a large number of other satellites which exhibit obviously different behavior. These satellites are very sharp lines, highly polarized, and grouped around the strongest electronic transitions of the RE ions. The properties held in common by these lines strongly suggest that they are all due to a common physical mechanism which is distinct from the ones described above. Such satellites have been observed in this laboratory[1] and others,[2] using other RE salts.

We have attempted to make a complete study of the properties of these Nd^{3+} satellites in RE trichlorides in an effort to ascertain their physical basis. Temperature dependence and Zeeman effect were studied as well as the effect of host lattices and impurity content. Several conceivable mechanisms have been considered in detail. While it is difficult to draw unambiguous conclusions, there are strong indications that the satellites are due to Nd^{3+} ions at irregular sites which are probably associated with crystal imperfections.

II. EXPERIMENTAL RESULTS

A. Experimental Details

We have investigated the satellite structure surrounding several of the strongest electronic transitions of Nd^{3+} in various host lattices. The following crystals, with their corresponding thickness, were examined: 1% $Nd{:}LaCl_3$(0.4, 1, 12.5 mm); 1% $Nd{:}PrCl_3$ (7 mm); 1% $Nd{:}GdCl_3$ (2 mm); $NdCl_3$ (0.1, 3, 10 mm); 1% $Pr{:}NdCl_3$ (3.5, 8 mm); 1% $Er{:}NdCl_3$ (3 mm). All of

---

* This research was supported in part by Atomic Energy Commission Contract No. AT(30-1)-1447 and National Aeronautics & Space Administration Grant No. NsG-361.

† Present address: U.S. Naval Research Laboratory, Washington, D.C.

‡ Present address: Bell Telephone Laboratories, Murray Hill, New Jersey.

[1] G. H. Dieke and L. Heroux, Phys. Rev. **103**, 1227 (1956).

[2] K. H. Hellwege, G. Hess, and H. G. Kahle, Z. Physik **159**, 333 (1960).

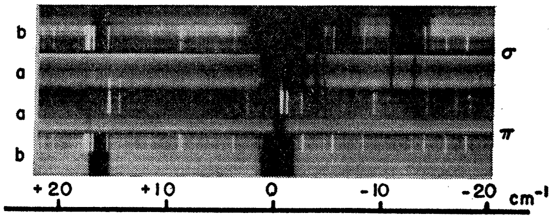

FIG. 1. The transition Z_1 ($^4I_{9/2}$)→E_1($^4G_{7/2}$) of Nd^{3+} at 4.2°K in (a) LaCl$_3$ and (b) NdCl$_3$. Only the σ, π line at the center is expected. The triple at +17 cm^{-1} in NdCl$_3$ is the ED forbidden transition Z_1 ($\mu=\pm\frac{5}{2}$)→E_2 ($\mu=\pm\frac{5}{2}$).

these samples except 1% Nd:PrCl$_3$[3] were produced in this laboratory by E. F. Williams.

All of the crystals investigated have the familiar UCl$_3$ structure.[4] They are hexagonal, having two molecules per unit cell, and the RE occupy a C_{3h} site. Each RE has two equivalent RE near neighbors (n-n) along the C_3 axis (optic axis). The usual convention is followed for describing the polarization of the absorption spectra: σ means $\mathbf{E}\perp C_3$ and π means $\mathbf{E} \parallel C_3$.

The techniques of obtaining low-temperature, high-resolution crystal absorption spectra in this laboratory have been thoroughly described elsewhere.[1] The spectra were recorded photographically on a 5-m, two-mirror Fastie spectrograph (Jarrell-Ash model 72360). It incorporates a 10-in. plane grating having 300 lines/mm, blazed at 5.9 μ, yielding a plate factor of 0.23 Å/mm at 5300 Å.

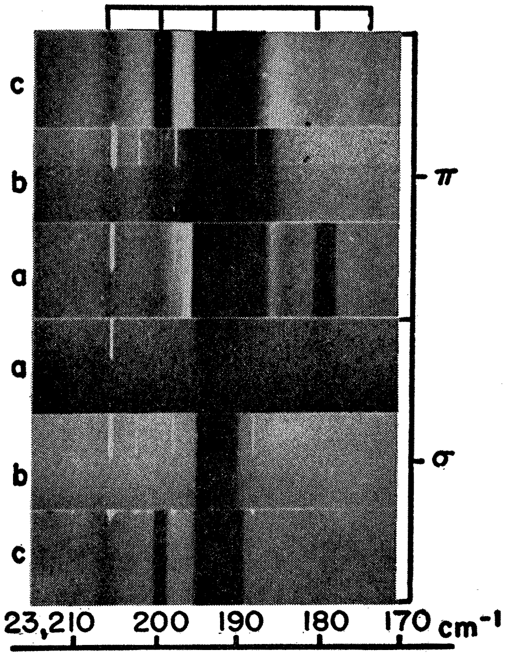

FIG. 2. The transition Z_1($^4I_{9/2}$)→I_1($^2P_{1/2}$) of Nd^{3+} at 4.2°K in (a) NdCl$_3$, (b) 1%Pr^{3+}/NdCl$_3$, and (c) 1%Er^{3+}/NdCl$_3$. Only the σ, π line at 23 193 cm^{-1} is expected.

Very thorough Zeeman studies were made with the external field parallel to the optic axis of the crystal sample. For samples of thickness ≥ 7 mm, the maximum field strength was 27.5 kOe, and for smaller samples it was 36 kOe. For the latter, the magnet has been calibrated to an uncertainty of ±150 Oe, and for the larger, to within ±200 Oe. A typical study would involve photographs for a single polarization with fields from 7 kOe up to the maximum at 1 kOe intervals.

Except for subsidiary experiments at 77 and 1.5°K to check upon temperature-induced variations in the spectra, the data were all taken at 4.2°K. These temperatures are the bath temperatures, and since these hygroscopic crystals are encapsulated in fused quartz tubing, their actual temperatures were somewhat higher. The tubing contained He at 300 to 600 mm pressure as an exchange gas. Interference filters with ≈100 Å bandpass were used with the light sources, so that the estimated temperature of the crystals was <5°K.

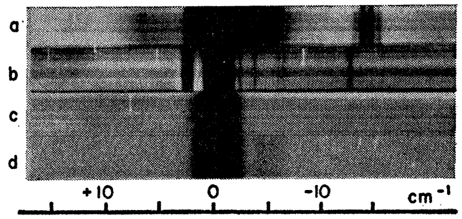

FIG. 3. The π component of the transition Z_1($^4I_{9/2}$)→I_1($^2P_{1/2}$) of Nd^{3+} at 4.2°K in (a) NdCl$_3$, (b) LaCl$_3$, (c) PrCl$_3$, and (d) GdCl$_3$. The samples for (b), (c), and (d) contain 1% dopings of NdCl$_3$.

Since the energy of the first excited state of Nd^{3+} in these crystals is ≈120 cm^{-1}, at this temperature we are only considering absorption from the ground state.

B. 1% Spectra

In this section, we shall discuss the observed features of the absorption spectrum of 1% Nd:LaCl$_3$. The principal features of this spectrum have been reported previously[5] where they have been analyzed on the basis of a crystalline field splitting of the Nd^{3+} ion in a C_{3h} site. There are, however, many additional interesting features of the spectrum which have not been reported. The most striking of these is the additional appearance of many weaker absorption lines. These lines, in general, are clustered about the well-known electronic transitions between the crystalline Stark levels. Some examples of this structure for Nd^{3+} are given in Figs. 1, 2, and 3.

---

[3] We are indebted to F. Varsanyi of Bell Telephone Laboratories for the use of this sample.

[4] Ralph W. G. Wyckoff, *Crystal Structures* (Interscience Publishers, Inc., New York, 1963), 2nd ed., Vol. II.

[5] E. H. Carlson and G. H. Dieke, J. Chem. Phys. **34**, 1602 (1961).

Table I. Satellite structure of selected electronic transitions of Nd^{3+} in LaCl$_3$ with Zeeman splittings.

$\Delta\nu$ cm^{-1} [a]	Pol.	Int.[b]	$\Sigma_{\parallel}{}^{+}$ [c]	$\Sigma_{\parallel}{}^{-}$
(a) $Z_1 \to A_1$ at 13 396.02 cm^{-1} $^4I_{9/2}$ ($\mu=\pm\frac{5}{2}$)$\to$$^4F_{7/2}$ ($\mu=\pm\frac{1}{2}$)				
0	π	···	+1.52	−1.52
0	σ	···	+2.60	−2.56
−11.05	π	1	0.87	
	σ	00		
−9.10	π	3	1.33	1.46
	σ	0	2.50	
−7.92	π	7	1.37	1.35
	σ	1	2.65	
−6.62	π	5	0.87	
	σ	0	3.00	
−6.11	π	2	0.98	
	σ	0		
−3.97	π	2	1.17	1.26
	σ	0		
−3.34	π	2	1.41	1.17
	σ	0		
−1.68	π	5	1.35	1.37
	σ	2	2.37	2.61
−1.12	σ	5	2.35	2.61
−1.07	π	0	1.39	1.52
−0.60	π	9		1.56
−0.57	σ	3	2.47	2.54
−0.44	π	9		1.47
−0.40	σ	6	2.47	2.56
−0.28	π	00	2.46	1.50
	σ	2		2.52
+0.11	σ	4		1.43
+0.48	σ	1		1.41
+0.54	π	9		1.50
	σ	6		2.63
+0.61	π	9	1.48	
	σ	8	2.59	
+1.03	π	9	1.43	
	σ	3	2.61	2.54
+5.74	π	5	1.24	1.26
	σ	0	2.71	
+8.08	π	0	1.54	1.30
	π	3	1.54	
+8.48	σ	0		
	π	3	1.56	1.37
	σ	0		
(b) $Z_1 \to A_2$ at 13 400.18 cm^{-1} $^4I_{9/2}$ ($\mu=\pm\frac{5}{2}$)$\to$$^4F_{7/2}$ ($\mu=\pm\frac{5}{2}$)				
0	π	···	−0.84	+0.59
0	σ	···	−3.30	+3.15
−3.13	π	5		0.96
	σ			0.74
	π	6	0.63	0.91
−0.36	σ	2	0.74	
	σ	1	3.12	
−0.18	σ	2	0.69	
+0.10	π	0	0.61	
	σ	0	3.15	
+0.77	π	8	0.67	0.83
	σ	3	3.20	3.20
+0.95	π	1	0.67	

$\Delta\nu$ cm^{-1} [a]	Pol.	Int.[b]	$\Sigma_{\parallel}{}^{+}$ [c]	$\Sigma_{\parallel}{}^{-}$
(c) $Z_1 \to D_1$ at 17 095.34 cm^{-1} $^4I_{9/2}$ ($\mu=\pm\frac{5}{2}$)$\to$$^4G_{5/2}$ ($\mu=\pm\frac{1}{2}$)				
0	σ	···	2.65	2.65
0	π	···	1.30	1.35
−18.61	σ	00		0.93
−18.14	σ	0		2.50
	π	0		1.33
−17.77	σ	00		0.93
−17.64	σ	0	2.72	2.72
	π	0	1.35	1.33
−10.94	π	1	1.15	1.48
	σ	00		2.52
−7.73	σ	00		2.85
	π	1		1.20
−6.27	π	0		1.35
−6.07	π	1		1.67
−5.84	π	1	1.80	
−2.47	π	2		
−2.04	π	0		
	σ	0	3.28	2.65
−1.72	σ	0	3.17	2.60
−1.64	π	0	2.04	
−1.44	π	4	1.41	
	σ	1	2.46	2.63
−1.14	π	9	1.22	1.35
−1.09	σ	5	3.04	2.65
−0.94	σ	00	3.04	
−0.69	σ	6	2.65	2.65
	π	9	1.33	1.35
−0.44	π	9	1.33	1.35
	σ	9	2.65	2.65
+0.48	π	9	1.35	1.35
	σ	3	2.65	2.65
+1.41	π	0		1.26
+1.46	σ	0	2.54	2.65
+1.81	π	9		1.33
+1.86	σ	0	2.43	
+2.09	σ	2		2.65
+2.36	π	4	2.65	2.52
+2.41	σ	5		1.33
+2.47	σ	00		
+2.61	σ	00		
+2.86	π	0		1.39
+3.74	σ	2		2.91
		4		1.63
+3.77	π	4		1.07
+4.68	π	0		3.13
+4.76	σ	2		0.98
+5.84	π	1		2.63
+6.75	π	0		
+9.41	σ			1.15
(d) $Z_1 \to E_1$ at 18 993.59 cm^{-1} $^4I_{9/2}$ ($\mu=\pm\frac{5}{2}$)$\to$$^4G_{7/2}$ ($\mu=\pm\frac{3}{2}$)				
0	σ	···	3.49	
0	σ	···	0.56	
0	π	···	0.52	0.54
−18.04	σ	00		
−14.02	σ	0	0.50	

TABLE I. (*Continued*).

$\Delta\nu$ cm^{-1} [a]	Pol.	Int.[b]	$\Sigma_{\|\|}^{+}$ [c]	$\Sigma_{\|\|}^{-}$
	(d) $Z_1 \rightarrow E_1$ at 18 993.59 cm^{-1} $^4I_{9/2}$ ($\mu=\pm\frac{5}{2}$)$\rightarrow G_{7/2}$ ($\mu=\pm\frac{3}{2}$) (*Continued*)			
−13.64	σ	4	0.54	0.52
	σ	2	1.00	1.11
−11.36	σ	6	0.52	0.46
	σ	2	0.93	
−10.29	π	00		
−9.64	σ	00		
−4.99	σ	00		
−4.60	σ	2	0.52	0.52
−4.10	σ	2	0.54	
−3.78	σ	3	0.56	
−3.52	σ	0	0.54	
−2.79	σ	00		
−2.41	σ	4	0.52	
−2.25	σ	7	0.54	0.52
−1.09	σ	9	0.56	
−0.67	σ	9		0.50
−0.44	π	2	0.46	
	σ	0	3.41	
−0.07	σ	0	3.49	
+0.33	π	0	0.63	
+0.81	σ	5	0.54	
+0.99	σ	5	0.54	
+1.13	σ	0	0.59	
+1.70	σ	3	0.56	

$\Delta\nu$ cm^{-1} [a]	Pol.	Int.[b]	$\Sigma_{\|\|}^{+}$ [c]	$\Sigma_{\|\|}^{-}$
	(e) $Z_1 \rightarrow I_1$ at 23 215.00 cm^{-1} $^4I_{9/2}$ ($\mu=\pm\frac{5}{2}$)$\rightarrow ^2P_{1/2}$ ($\mu=\pm\frac{1}{2}$)			
0	σ	...	2.24	2.30
0	π	...		1.70
−12.75	π	4	1.70	1.65
−6.58	π	1	1.70	1.61
−6.07	π	1	1.70	1.59
−4.91	π	0	1.65	1.67
−3.86	π	2	1.67	1.66
−2.48	π	3	1.70	1.67
−1.99	π	0		1.22
−1.10	σ	0	2.28	2.22
−0.93	π	9	1.76	1.65
−0.72	σ	0	2.30	2.15
−0.67	π	9	1.76	1.74
−0.44	π	9	1.76	1.65
+0.47	π	9		1.76
+0.53	σ	0	2.29	1.93
+0.75	π	0	1.87	1.67
+1.23	π	2	1.70	1.67
+1.28	σ	0		
+1.59	π	0	1.74	1.61
+2.08	π	9	1.72	1.70
+2.12	σ	2	2.30	
	π	9	1.74	1.70
+2.52	π	9	1.74	1.70
	σ	2	2.26	
+2.56	π	9	1.70	1.70
+2.84	π	0	1.70	

[a] The braces indicate lines which were apparent doubles.

[b] The parent lines were, in all cases, overabsorbed, but estimates of their strength based upon linewidth indicates they are from 10^4 to 10^5 stronger than the intensity 1. Intensity 10 indicates onset of overabsorption; 00 is the limit of detectability.

[c] $\Sigma_{\|}^{+}$ and $\Sigma_{\|}^{-}$ are the normalized slopes of the Zeeman patterns versus fields, toward increasing and decreasing wave numbers respectively, in Lorentz units.

The following general features of this satellite structure have been observed:

(1) They are only found clustered about an electronic transition line, never more than ≈20 cm^{-1} away.

(2) They are usually more plentiful on the short-energy side of the "parent" line, and extend farther away on that side.

(3) The number and intensity of the satellites increase with sample thickness. There is, however, an apparent limit to the number, so that increasing sample thickness beyond a point (≈10 mm) will continue to enhance the intensity of the satellites, but will not bring any new ones to view.

(4) The intensities of the satellites are observed to be 10^{-3} to 10^{-4} of their "parent" line, and they show no systematic dependence upon the displacement from the parent line. This was obtained for the transition $Z_1 \rightarrow I_1$, and it is accurate to within an order of magnitude. There are few exceptionally strong satellites (with intensity of 10^{-1}–10^{-2} of the parent lines) on the higher energy side of the parent transition.

(5) The satellites are generally very sharp, having linewidths of ≈0.05 cm^{-1}.

(6) They are found only about the strongest and sharpest of the electronic transitions. Because of the well-known phonon broadening of the crystal levels, this meant that they were usually found only about the transitions to the lowest member of any Stark manifold.

(7) Most of the satellites were completely polarized, either σ or π. This is illustrated in Figs. 1 and 2. This property appears to be intimately connected with item (6) above, in that when the parent line was allowed in both polarizations it was usually much stronger in one than it was in the other. Likewise, the satellites associated with that line would appear almost exclusively in the stronger polarization.

(8) From Figs. 1 and 3, one can observe an apparent tendency for the satellites to occur as pairs, both members of a pair having approximately the same intensity and linewidth. Separations between pair members range from 2.28 cm^{-1} to 0.1 cm^{-1}.

(9) There appears to be no regular relation among the spacings of the satellites, nor is there any repeated pattern of satellites independent of the parent line.

(10) For the parent lines studied, there was no departure from linearity in the Zeeman patterns, and this property was shared by the satellites.

(11) Most of the satellites split in an applied parallel magnetic field at the same rate as the parent line in a given polarization. (See entries in Table I.)

(12) There were some cases in which the σ component of a satellite would split as the π component of the parent, and vice versa.

(13) There were cases in which a satellite in only one polarization would exhibit a complete four-line Zeeman pattern.

(14) There were cases in which the satellite splitting was different from that of the parent. When σ, π components of such lines were observable, it was found that they gave the correct ground-state splitting factor, but the other splitting factor did not agree with that of the upper level corresponding to the parent line.

Most of the above observations can be verified from data in Tables I and II. The energies, intensities, polarizations, and Zeeman splittings of the satellites and their parent lines are listed here. The uncertainty in the values of $\Delta\nu$ are, in general, ± 0.05 cm^{-1}. The lines in LaCl$_3$ were always sharper than those in NdCl$_3$, hence strong lines (Int.>5) in LaCl$_3$ could be measured to ± 0.01 cm^{-1}, while weak lines in NdCl$_3$ (Int.<2) could be measured to only ± 0.1 cm^{-1}. Complete entries for only five parent transitions are recorded. Although satellites were observed for twice that number of parents, due to the time restrictions for the lengthy Zeeman studies, the ultraviolet and infrared extremes of the photographic region were not completely investigated. One may note that the Zeeman splittings were the evidence which enabled us to properly allocate the components of the overlapping satellite patterns of A_1 and A_2 as shown in Table I(a) and (b).

The observed satellites were found to be independent of the samples used. The 1-mm sample had been grown and cut about 5 yr before the measurements were taken, and the other samples were cut from different boules grown about 2 yr before. A study was then made of the dependence of these satellites upon the host lattice. The inert closed shell La^{3+} ions were replaced in turn by first Pr^{3+}, then Gd^{3+}, and finally Nd^{3+}. Since LaCl$_3$, PrCl$_3$, NdCl$_3$ and GdCl$_3$ are isomorphic, and any will accept any of the others in any concentration, any variations in the spectra must be due to interaction of the Nd^{3+} ions with the RE ions of the host. A typical result is shown in Fig. 3. The most impressive point, of course, is that "active" RE neighbors tend to drastically alter the intensities of the satellites. In PrCl$_3$ and GdCl$_3$ some of the satellites are completely quenched. In NdCl$_3$ they are much weaker, especially when one considers the intensity relative to the number of Nd^{3+} ions in the absorption path when one goes from 1% Nd:LaCl$_3$ to 100% NdCl$_3$ crystals of equal thickness. The other important observation is that the satellites in NdCl$_3$ have considerable structure of their own, so that instead of appearing in pairs, they appeared as triples or quadruples.

C. 100% NdCl$_3$

As reported recently,[5] the spectrum of NdCl$_3$ (aside from the satellite structure) differs from that of Nd^{3+}:LaCl$_3$ in only one important respect. Each single electronic absorption line in LaCl$_3$ acquires a triple structure in the pure salt. This was readily analyzed on the basis of $J_{ij}S_{iz}S_{jz}$ nearest-neighbor (n-n) interactions between Nd^{3+} ions. Now in the satellite structure we observe a similar enrichment of the line structure in going from a LaCl$_3$ matrix to pure NdCl$_3$. This is illustrated in both Figs. 1 and 3.

Table II. Satellite structure of selected electronic transitions of Nd^{3+} in LaCl$_3$ without Zeeman splitting.

$\Delta\nu$ cm^{-1} [a]	Pol.	Int.[b]
(a) $Z_1 \rightarrow R_1$ at 11 423.85 cm^{-1}; $^4I_{9/2}$ ($\mu=\pm\frac{5}{2}$)$\rightarrow$$^4F_{3/2}$ ($\mu=\pm\frac{1}{2}$)		
-12.62	π	0
-10.77	π	0
-7.77	π	6
	σ	5
-5.76	π	6
	σ	5
-4.78	π	00
-4.19	π	00
-3.67	σ	4
-3.10	π	5
	σ	3
-2.86	π	5
	σ	3
-1.84	π	4
	σ	1
-1.60	π	4
	σ	1
-1.23	π	00
	σ	00
$+1.41$	π	00
	σ	00
(b) $Z_1 \rightarrow S_1$ at 12 458.31 cm^{-1} $^4I_{9/2}$ ($\mu=\pm\frac{5}{2}$)$\rightarrow$$^4F_{5/2}$ ($\mu=\pm\frac{1}{2}$)		
-8.38	π	7
	σ	4
-7.60	π	0
	σ	0
-6.20	π	3
-6.07	σ	3
-5.39	π	3
	σ	3
-3.90	π	3
	σ	3
-2.20	π	3
	σ	3
-1.62	π	00
	σ	00
$+1.56$	π	00
$+1.79$	π	2
$+2.02$	σ	00
$+2.43$	σ	00

[a] The braces indicate lines which were apparent doubles.

[b] The parent lines were, in all cases, overabsorbed, but estimates of their strength based upon linewidth indicates they are from 10^4 to 10^5 stronger than the intensity 1. Intensity 10 indicates onset of overabsorption, 00 is the limit of detectability.

TABLE III. Satellite structure of selected electronic transitions of Nd^{3+} in $NdCl_3$ with Zeeman splitting.

$\Delta\nu$ cm^{-1} [a]	Pol.	Int.[b]	$\Sigma_{\parallel}^{+}$ [c]	$\Sigma_{\parallel}^{-}$
(a) $Z_1 \rightarrow I_1$ at 23 193.31 cm^{-1}; $^4I_{9/2}\ (\mu=\pm\frac{5}{2}) \rightarrow {}^2P_{1/2}\ (\mu=\pm\frac{1}{2})$				
0	π	···	2.4	2.4
0	σ	···		
−14.61	π	1	1.85	1.87
(−14.11)	σ	00	2.35	
−13.75	π	9	1.91	1.93
(−13.32)	σ	00	2.33	
−13.01	π	9	1.93	1.93
(−12.61)	σ	00		
−12.41	π	1	1.83	1.87
−6.19	π	2		1.89
−5.59	π	9	1.72	1.83
−4.97	π	9	1.72	1.74
(b) $Z_1 \rightarrow E_1$ at 18 974.20 cm^{-1}; $^4I_{9/2}\ (\mu=\pm\frac{5}{2}) \rightarrow {}^4G_{7/2}\ (\mu=\pm\frac{3}{2})$				
0	σ	···	0.63	
0	π	9	3.67	
−14.68	σ	3	0.67	
−14.03	σ	0		
−13.09	σ	9	0.67	
−12.22	σ	0		
−11.23	σ	9	0.76	
−10.23	σ	0		
−9.60	σ	3	0.87	
−8.20	σ	0	0.61	
−7.68	σ	3	0.72	
−6.85	σ	9	0.65	
−6.08	σ	9	0.61	
−5.72	σ	0	0.78	
−5.14	σ	3	0.65	
−3.83	σ	0	0.70	
(c) $Z_1 \rightarrow A_1$ at 13 384.13 cm^{-1} $^4I_{9/2}\ (\mu=\pm\frac{5}{2}) \rightarrow {}^4F_{7/2}\ (\mu=\pm\frac{1}{2})$				
0	π	···		1.65
0	σ	···	2.74	2.80
−11.05	π	0	1.71	
−10.18	σ	00	2.61	
−10.13	π	1	1.63	
−9.51	π	1	1.66	
−8.74	π	0	1.67	1.78
−7.64	π	0	1.62	
−6.88	π	0		
−6.20	π	0		
−5.14	π	0		
−4.44	σ	1		
−4.39	π	1		
−3.66	π	1		
	π	1		
	σ	1		
−2.91	σ	0		

[a] The braces indicate lines which were common members of an apparent triple or quadruple; parentheses indicate that the position was determined from the slope of the lines versus magnetic field.

[b] The parent lines were, in all cases, overabsorbed, but estimates of their strength based upon linewidth indicates they are from 10^4 to 10^5 stronger than the intensity 1. Intensity 10 indicates onset of overabsorption, 00 is the limit of detectability.

[c] $\Sigma_{\parallel}^{+}$ and $\Sigma_{\parallel}^{-}$ are the normalized slopes of the Zeeman patterns toward increasing and decreasing wave numbers respectively, in Lorentz units.

Figure 3 shows a very prominent quartet which is the most common grouping of satellites in the pure salt (just as doubles were the most common feature of the satellite spectrum in $LaCl_3$). This figure also shows how the crowded satellite structure in the pure salt, merging into the parent line, gives rise to the apparent excessive line breadths in the pure salt.

Figure 1 provides a further comparison. The polarization of the satellites is complete in both salts. The center of the farthest double in $LaCl_3$ has the same displacement from the parent line as does the quadruple in $NdCl_3$. In addition, the quadruple is symmetrically interlaced with a diffuse triple. In a parallel magnetic field, all components split at the same rate as the σ component of the parent line [see Table III]. This example of a joint appearance of triple and quadruple is not unique. In the other two examples ($Z_1 \rightarrow S_1$ and $Z_1 \rightarrow I_1$) the triple and quadruple are observed in opposite polarizations, and the Zeeman splittings follow the parent lines. [See Tables III and IV.]

In summation, the observed spectra suggest that the mechanism responsible for the large shifts away from the parent line is probably the same in both $LaCl_3$ and $NdCl_3$ and only the finer structure (singles and doubles, versus triples and quadruples) is dependent upon the identity of neighboring RE ions.

Aside from the foregoing comments, the observations listed for 1% Nd:$LaCl_3$, hold true for $NdCl_3$ satellites. In addition, we note the following detailed behavior of the quadruple fine structure in an applied parallel magnetic field as illustrated in Fig. 4. The behavior is very similar to that of the triple structure of the parent lines as is fully described in Ref. 5 (except that unlike the satellite's fine structure in a perpendicular magnet field, the triple structure of the main line is obliterated). The four lines each split linearly into two components, the quadruple spacings remaining unchanged for each set. The low-energy quadruple suffers in intensity with increasing field while the high-energy one is enhanced. Furthermore, within each, the intensity shifts from the outside of the pattern toward the inside. Ultimately, in high field, only the inside components survive, the high-energy side being much stronger than the low-energy side. One also observes a considerable sharpening of the components with increasing field (an effect also achieved by lowering the temperature). Finally, one observes a general deterioration of the satellites in the pure salt, the lines becoming both less numerous and less sharp than those in $LaCl_3$.

All of these observations are very reminiscent of those made of the parent line and suggests a similar explanation—namely, interactions between neighboring Nd^{3+} ions. This will be discussed later.

Finally, we investigated the effect that other RE impurities would have upon the satellites in $NdCl_3$. As shown in Fig. 2, 1% impurities of either Pr^{3+} or Er^{3+} had an extraordinarily dramatic influence. The satellites almost vanish entirely. This influence was observed to be uniformly effective throughout the spectrum, although Pr^{3+} was a somewhat more effective agent that Er^{3+}.

D. Additional Experiments

The temperature dependence of these lines was investigated both by pumping upon the helium bath and using a liquid-nitrogen bath. At these bath temperatures of 1.5 and 77°K, the intensities of the satellites relative to the parent line were unaffected. At the lower temperature, both the parents and satellites sharpened; at the higher temperature, they both broadened.

We also compared the spectra of $NdCl_3$ taken with a highly filtered source necessitating exposures of 100 min, with those of an unfiltered source allowing exposures of 1 min, all other experimental conditions remaining the same. The approximately two orders of magnitude change in the intensity of the source had no effect upon the spectra. This was done to rule out any possible dependence of the satellites upon the population of ions in the excited state of the parent line.

Finally, the possibility of the existence of any significant population of an excited state under our experimental conditions was investigated, since such ions could conceivably give rise to the satellites via ion-pair interactions. Varsanyi has shown that it is possible to pump the longest-lived metastable state $Y_1(^4I_{11/2})$, which in $PrBr_3$ has a lifetime of 100 msec.[6] We chose an excited state which was connected to Y_1 by a strong transition probability, as evidenced by strong fluorescence. This was $L_1(^4D_{3/2})$. Then using carefully filtered light to prevent populating L_1 or higher states, thus avoiding $L_1 \rightarrow Y_1$ fluorescence which could mask any observed $Y_1 \rightarrow L_1$ absorption, no trace of such absorption was observed. Hence, it was concluded there was no significant population of any excited states.

TABLE IV. Satellite structure of selected electronic transitions of Nd^{3+} in $NdCl_3$ without Zeeman splitting.

$\Delta\nu$ cm^{-1} [a]	Pol.	Int.[b]
(a) $Z_1 \rightarrow R_1$ at 11 414.25; $^4I_{9/2}$ $(\mu=\pm\frac{5}{2}) \rightarrow {}^4F_{3/2}$ $(\mu=\pm\frac{1}{2})$		
−9.67	π	0
−8.54	π	1
−7.33	π	00
−6.69	π	2
−5.44	π	2
−4.18	π	0
−3.78	π	0
−2.98	π	2
−1.95	π	0
	σ	00
−1.76	π	00
+1.80	π	00
+2.15	π	0
+2.32	σ	00
(b) $Z_1 \rightarrow S_1$ at 12 447.62. $^4I_{9/2}$ $(\mu=\pm\frac{5}{2}) \rightarrow {}^4F_{4/2}$ $(\mu=\pm\frac{1}{2})$		
−10.10	π	0
−9.96	σ	1
−9.23	σ	2
−9.12	π	1
−8.82	π	4
−8.60	σ	1
−8.41	π	1
−7.40	σ	1
−6.75	σ	0
−6.52	π	1
−6.26	σ	1
−5.16	π	00
−4.94	σ	2
−4.48	σ	1
−4.43	π	0
−3.70	σ	0
−3.57	π	0
−2.72	σ	1
−2.21	σ	00
−2.12	π	00
+2.15	π	00
+2.25	σ	00

[a] The braces 4 indicate lines which were apparent doubles.

[b] The parent lines were, in all cases overabsorbed, but estimates of their strength based upon linewidth indicates they are from 10^4 to 10^5 stronger than intensity 1. Intensity 10 indicates onset of overabsorption, 00 is the limit of detectability.

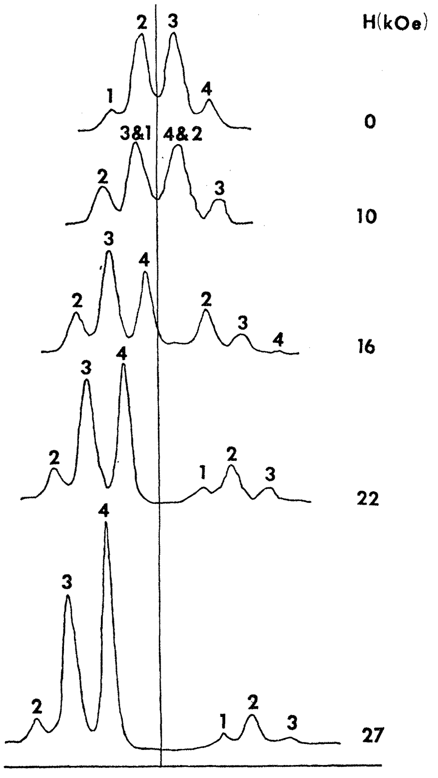

FIG. 4. Zeeman splitting of the quadruple satellite of the π transition $Z_1(^4I_{9/2}) \rightarrow I_1(^2P_{1/2})$ of Nd^{3+} in $NdCl_3$ at 4.2°K. The applied magnetic field was parallel to C_3.

III. DISCUSSION

It is obvious that the system of a single RE ion, situated at its normal site in the crystal, and unaffected by crystal vibrations, can give rise to only a unique set

---

[6] F. Varsanyi, Bull. Am. Phys. Soc. **12**, 293 (1967).

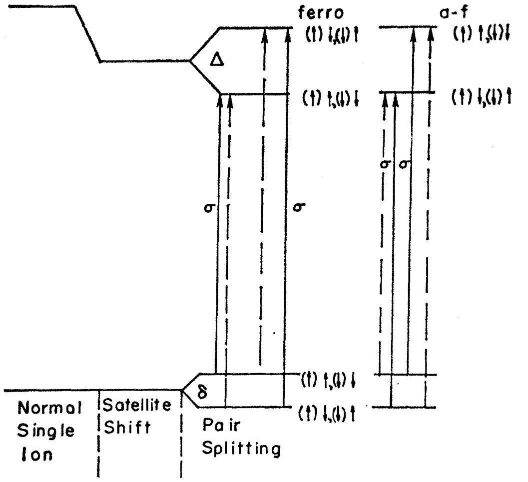

FIG. 5. Energy-level diagram of coupled Nd^{3+} pair assuming either ferromagnetic coupling or antiferromagnetic coupling between ions in the upper state. The observed σ transitions are solid lines, the unobserved transitions are dashed lines.

of energy levels. It is necessary, therefore, to search for additional irregular conditions in which the RE ion can be found and which give rise to the observed spectra. The occurrence of such conditions is very improbable, as indicated by the relative intensities of the satellites to their parent transitions. Furthermore, these irregular conditions differ only slightly from those of the normal Nd^{3+} environment. This is indicated by the following observations: the fact that the satellites accompany the strongest transitions thus relate their transition strengths to those of the parents. Weak electronic transitions exhibit no satellites. Also, in most cases, the Zeeman-splitting factor of the satellite is either equal to that of the main line or only slightly different from it. Since for all but one of the transitions studied, the upper state was composed of only one m_j value, while the ground state is a mixture of $m_j = \pm\frac{5}{2}, \pm\frac{7}{2}$; this may indicate that the shifts are due to perturbations of the upper states. Rather striking is the fact that the farthest-removed satellites have the polarization of the stronger component of their parent. This effect is observed for all groups studied here, for both dilute and concentrated crystals. For Nd^{3+} in $RECl_3$, as a consequence of electric dipole selection rules, all σ transitions between $\mu=\pm\frac{5}{2}$ states and $\mu=\pm\frac{1}{2}$ states involve a change in the sign of the ion's magnetic moment, while the π transitions do not. For the transitions $\mu=\pm\frac{5}{2}\rightarrow\mu=\pm\frac{3}{2}$ the σ components (which are the only ones allowed) do not involve such a change. Throughout the spectrum, the "no-moment flip" transitions are usually the stronger, hence they are accompanied by most of the satellite structure.

A comparison between the separations of the satellites associated with different parent transitions reveals that only a small number of them have a common separation from the parent. Because of this, and the lack of any other systematic distinguishing features, there is no clear way to associate the satellite of one electronic transition with that of another. Furthermore, the unavailability of satellites with all the components of some Stark manifold prohibits separating out the satellites according to their respective sources. Generally, the satellites are observed with the lowest Stark component of a group due to its sharpness. The broadening of the upper components presumably results in a broadening of the satellites which thus escape detection.

A good deal of information is contained in the detailed structure of the satellites. Consider first the diluted crystal. Those satellites which appear in pairs can be attributed to a pair of Nd^{3+} ions. The pair of satellites separate by -13.64 and -11.36 cm^{-1} from the transition ${}^4I_{9/2}(\mu=\pm\frac{5}{2}) \rightarrow {}^4G_{7/2}(\mu=\pm\frac{3}{2})$ serves as an example. The two lines are close in intensity and polarization. (They correspond to a structure of four strong lines interlaced with three weak lines in the 100% $NdCl_3$ crystal). Their Zeeman effect is similar: one component arises from the lower ground-state component, $\mu=\frac{5}{2}$, and it is enhanced with increasing H. The other arises from the upper component $\mu=-\frac{5}{2}$ and it diminishes with increasing field. These components have the same slopes of magnetic energy versus magnetic field (Σ) as the parent transitions. From the observed spectrum of triples in $NdCl_3$,[7] we know that the interaction energy for a Nd^{3+} pair is 0.35 cm^{-1} for the ground state. If we assume that this is the case for a pair of Nd^{3+} ions in $LaCl_3$, we conclude that there must be a larger interaction when one of them is in the excited state in order to give rise to the observed double indicated in Fig. 5. The observed transitions are marked with solid lines while the (presumed) unobserved ones with dashed lines. The intensity difference between the two observed lines is not at variance with the ratio of populations of the ground-state components, $\exp\{-\delta/kT\}$. The fact that the intensity ratio is maintained with increasing magnetic field agrees well with the assumption that the transitions are observed from the two components of the pair ground state. Lacking the information from the other polarization, the sign of the coupling for the upper state is undetermined.

We turn our attention now to the $NdCl_3$ crystal and consider the observed quadruple structure, assuming that the same (as yet unknown) mechanism is responsible for the shifts as in the dilute crystal. In $LaCl_3$, the splitting is attributed to the Nd^{3+} ion having one peculiar neighbor—namely, another Nd^{3+} ion. Here again, we assume the structure to arise from interaction with one peculiar neighbor. Since here, both n-n are Nd^{3+} ions, the peculiarity is attributed to one of them. From this assumption, the energy-level diagram presented in Fig. 6 follows immediately. The observed transitions are then indicated on this diagram.

---

[7] G. A. Prinz, Phys. Rev. 152, 474 (1966).

With a parallel external magnetic field applied, the population of those neighborhoods having moments parallel to the field will be enhanced at the expense of antialigned neighborhoods. A comparison of the observed spectrum (Fig. 4) is in agreement with this proposed scheme. The experimental observation of an interlacing triple (either in the same or in the other polarization) is at odds with this description. It should be noted, in Fig. 6, that if one considers both neighbors to be normal for the ground state, then the ground state will exhibit the normal threefold splitting. This combination of a threefold splitting and a fourfold splitting in the excited state will still result in an observed quadruple. In order to explain the interlaced triple, one could envision that intrinsic to the quadruple transitions is the creation of a peculiar neighbor while those of the triple transitions do not. This idea of the ground state being normal is supported by observation 14 of Section IIB, concerning the ground-state splitting factor.

There remains the additional possibility of attributing the fourfold splitting to the interaction of an ion with three neighbors. While this is unreasonable in a normal RE site (having two n-n), two of the allowed interstitials, having C_{3h} symmetry, have three equidistant coplanar neighbors. The resulting energy-level diagram is straightforward and predicts the observed quadruple structure and the observed Zeeman behavior. It, however, leaves no possibility of observing a triple without additional artificial restraints, demanding energy coincidences.

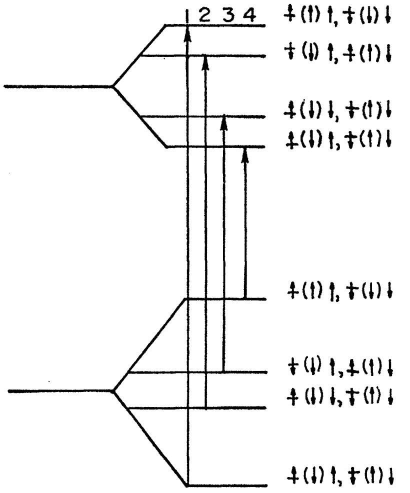

FIG. 6. Energy-level diagram of Nd^{3+} in vicinity of one regular ion (plain arrow) and one peculiar ion (crossed arrow). During an optical transition only the ion itself (in parenthesis) may change its state, the neighboring ions remaining unchanged. The diagram labeling assumes antiferromagnetic coupling to both neighbors in both states. If the coupling were of equal magnitude, the fourfold splitting would reduce to a symmetric threefold splitting. The numbered transitions correspond to the numbers in Fig. 4.

We shall now consider mechanisms which may be operative in the crystalline environment so as to cause satellite lines. The predictions based upon these mechanisms shall be compared with the observations.

The normal optical spectrum of RE trichlorides is due to single ions located at sites of C_{3h} symmetry. Additional optical transitions can arise from ions located at sites of other symmetries. The strong polarization shown by the satellites could indicate that if they are due to ions at irregular sites (then the site symmetry is relatively high), or that hidden selection rules are operative. The possible interstitial site symmetries found in the RE trichlorides unit cell are C_{3h}, C_{3i}, C_3, C_s, C_i, and C_1.

A given electronic state of an ion with an odd number of electrons, located at a C_3 site, can be characterized by one of the following irreducible representations: Γ_4 $(\mu=+\frac{1}{2})$, Γ_5 $(\mu=-\frac{1}{2})$, or Γ_6 $(\mu=\pm\frac{3}{2})$. The selection rules for electric and magnetic dipole transitions are: $\Gamma_{4,5}\leftrightarrow\Gamma_{4,5}$ is $\sigma\pi$; $\Gamma_{4,5}\leftrightarrow\Gamma_6$ is σ; $\Gamma_6\leftrightarrow\Gamma_6$ is π. Since a $J=\frac{1}{2}$ state of free ion becomes $\Gamma_{4,5}$ in the crystal, by the above selection rules, transitions to such a Kramer's doublet from any crystal level can never be π only. But as can be seen from Table I(e), most of the satellites of $Z_1\rightarrow I_1$ are π polarized. This, however, does not exclude the possibility of Nd^{3+} ions at C_3 sites being a source for some satellites. It is well known that except for symmetry selection rules, some additional ones can be operative as a result of the particular composition of an ionic state. Similar considerations can be applied to ions at C_{3i} sites. Since $C_{3i}=C_3\times C_i$, only magnetic dipole transitions are allowed within a configuration, the center of inversion prohibiting electric dipole transition. These states are characterized by $\Gamma_{4,5}^-$ or Γ_6^- and the symmetry selection rules are the same as those for C_3. Except for the regular C_{3h} sites occupied by the RE ions there are two other sets of interstitial C_{3h} sites in the unit cell. These will give rise to the same symmetry selection rules as apply to the regular ions. And, finally, the sites of lower symmetry C_s and C_i will give rise to unpolarized spectra. However, it should be emphasized again that symmetry selection rules are not always the only ones which are operative and, therefore, do not rule out the possibility of ions at irregular sites as a source for the satellites.

Similarly, RE ions at normal sites with a vacancy (of a Cl^- or another RE ions) in the close neighborhood can give rise to a satellite structure. Again, although the site symmetry is lower than C_{3h}, the resulting spectra could nevertheless show some polarization.

A remaining possibility is gross imperfections such as dislocations. There are many irregular sites in the vicinity of such imperfections. One can expect that these sites will exhibit a wide range of crystalline environments, i.e., various symmetries and field strengths. While the number and character of such imperfections depend on the conditions of growth, even in wellannealed crystals they are common. Since all the crystals studied here were produced in this laboratory under similar conditions, one could expect the nature of their imperfections to be similar.

As is well known from the theory of dislocations in metals,[8] there is an affinity between dislocations and impurities. This is a result of the distortion of lattice sites near the dislocation, resulting in an attraction of larger ions to larger sites and smaller ions to smaller sites. Also, introduction of impurities can induce dislocations in an otherwise pure crystal. From this, several of the observed facts can be understood. First, the relative intensities of the satellites of Nd^{3+} in $LaCl_3$ are expected to be higher than in $NdCl_3$ [see Sec. II(C)]. The mere introduction of Nd^{3+} in $LaCl_3$ can induce more dislocations, and in the process of growth, the dislocations will tend to migrate to the dopant ions. Hence, the relative number of ions at irregular sites will be higher for Nd^{3+} in $LaCl_3$ than for $NdCl_3$. Impurities (such as Pr^{3+}, Er^{3+}) which are introduced into $NdCl_3$ will tend to occupy the irregular sites, displacing the Nd^{3+} ions, and thus reducing the intensity of the Nd^{3+} satellites. As illustrated in Fig. 1, the satellites of Nd^{3+} in $PrCl_3$ and $GdCl_3$ are highly quenched. The reason for this is most probably due to a different mechanism, namely, the diffuse broad character of all the Nd^{3+} transitions due to ion–ion interactions.

Another consequence of the affinity of impurities to dislocations is the observed appearance of doubles in the satellite spectrum of Nd^{3+} in $LaCl_3$. In the undistorted regions of the crystal, one could expect the Nd^{3+} distribution to be random with a correspondingly low probability for n-n pairs. The relatively higher concentration in the vicinity of dislocations makes pairs more probable. Hence, we have the appearance of doubles as well as single lines among the satellites. Similarly, one can envision the occurrence of triples and quadruples in pure $NdCl_3$. If the ion undergoing an optical transition has two similar near neighbors, it will give rise to a triple structure, while if the near-neighbor sites are unequally distorted, the resulting structure could be a quadruple. In any case, the shift from the parent line is due to the local distorted crystalline field. The magnitude of the shifts ($\approx 10\ \mathrm{cm}^{-1}$) is consistent with this picture, while it is far too large to be attributed to near-neighbor interactions. The observed convergence of the spectral pattern towards the parent line is consistent with a series of irregular sites with decreasing amount of distortion. The most distorted sites, giving rise to the most distant satellites, will be those located nearest the dislocation. As one draws away from the dislocation, the distortion decreases, but one has an increasingly larger variety of sites available. Hence, as the satellites approach the parent line, they become more numerous.

There remain details of the spectra (such as the interlaced triple-quadruple in pure $NdCl_3$ or the preponderance of satellites on the low-energy side of the parent line) whose complete understanding depends upon a detailed knowledge of the nature of the distortions. A systematic study of imperfections in these crystals would thus aid materially in the understanding of the observed spectra, and hopefully would lead to the association of specific spectral lines with specific types of imperfection.

IV. SUMMARY

The high-resolution spectroscopic studies made here of the sharp satellite structure surrounding the electronic transitions of Nd^{3+} in $LaCl_3$ and $NdCl_3$ indicate that these transitions arise from ions in irregular sites. In particular, the extreme sensitivity of the intensity of these lines to host lattice and impurities strongly suggests that these irregular sites are associated with crystal dislocations, and with the tendency for dislocations to attract impurity ions. The structure of the satellite lines is found to be indicative of n-n interactions, and is taken to be further evidence for both clustering of impurity ions, and the distortion of neighboring rare-earth sites.

ACKNOWLEDGMENTS

We would like to thank Professor H. M. Crosswhite, and Professor H. W. Moos for their support and encouragement of this work, and Professor B. R. Judd for many helpful discussions. A special debt is owed J. Conquest for her painstaking measurements of the spectra. For the rendering of the typescript, we thank J. Foehrkolb.

---

[8] A. H. Cottrell, *Dislocations and Plastic Flow in Crystals* (Oxford University Press, London, 1953).

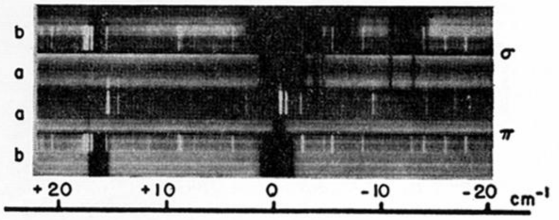

FIG. 1. The transition Z_1 $(^4I_{9/2})\rightarrow E_1(^4G_{7/2})$ of Nd^{3+} at 4.2°K in (a) $LaCl_3$ and (b) $NdCl_3$. Only the σ, π line at the center is expected. The triple at $+17$ cm^{-1} in $NdCl_3$ is the ED forbidden transition Z_1 $(\mu=\pm\frac{5}{2})\rightarrow E_2$ $(\mu=\pm\frac{5}{2})$.

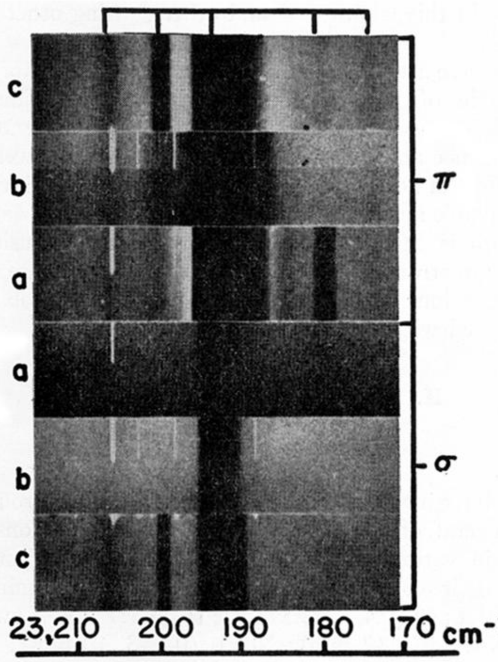

FIG. 2. The transition $Z_1(^4I_{9/2})\rightarrow I_1(^2P_{1/2})$ of Nd^{3+} at 4.2°K in (a) NdCl$_3$, (b) 1%Pr^{3+}/NdCl$_3$, and (c) 1%Er^{3+}/NdCl$_3$. Only the σ, π line at 23 193 cm^{-1} is expected.

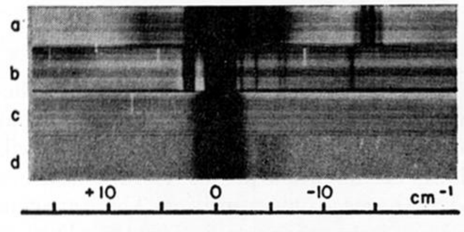

FIG. 3. The π component of the transition $Z_1(^4I_{9/2})\rightarrow I_1(^2P_{1/2})$ of Nd^{3+} at 4.2°K in (a) $NdCl_3$, (b) $LaCl_3$, (c) $PrCl_3$, and (d) $GdCl_3$. The samples for (b), (c), and (d) contain 1% dopings of $NdCl_3$.